Available online at www.sciencedirect.com
ScienceDirect
Sensors and Actuators A 133 (2007) 311–316
SENSORS AND ACTUATORS A PHYSICAL
www.elsevier.com/locate/sna

Surface nanostructuring by femtosecond laser irradiation through near-field scanning optical microscopy

Y. Lin [a,b,c], M.H. Hong [a,b,*], W.J. Wang [a], Z.B. Wang [a], G.X. Chen [c], Q. Xie [a], L.S. Tan [b], T.C. Chong [a,b]

[a] *Data Storage Institute, Singapore*
[b] *Department of Electrical and Computer Engineering, National University of Singapore, Singapore*
[c] *Nanoscience & Nanotechnology Initiative, National University of Singapore, Singapore*

Received 8 July 2005; received in revised form 10 March 2006; accepted 11 May 2006
Available online 25 July 2006

Abstract

A near-field scanning optical microscopy (NSOM) and a double-frequency femtosecond laser (400 nm, 100 fs) were applied to push the optical resolution further down to sub-50 nm on thin UV photoresist. A 20-nm feature size can be obtained. It is at a resolution of λ/20 (λ: laser wavelength) and *a*/2 (*a*: NSOM probe aperture diameter), respectively. It is proved that laser power and exposure time can affect feature size of lithography patterns. In this paper, the effect of probe-to-sample distance on dot-pattern features is studied, and different dot-pattern shapes are generated: dumbbell-dot, ellipsoid-dot and circle-dot. The simulated light field spatial distributions across the nano-aperture based on Bethe–Bouwkamp model is found to agree with experimental results very well.

Keywords: Near-field scanning optical microscopy; Femtosecond laser; Bethe–Bouwkamp model

1. Introduction

During the last two decades, there has been an upsurge of interest in ultrahigh-capacity optical data storage. The field of optics is entering an exciting new phase due to the rapid development of near-field optical techniques, such as near-field scanning optical microscopy (NSOM). It offers a high resolution to overcome the optical diffraction limit [1], which is one of the main bottle necks in further development of optical microscopy, optical projection lithography, integrated optics, and optical data storage. Due to small optical fiber probe aperture and short probe-to-sample distance at a scale of dozens of nanometers, there is high enough intensity of evanescent light across the fiber probe arriving onto the sample surface before disappearing. On the other hand, the rapid development of femtosecond lasers over the last decade has opened up a wide range of new applications in material science and has been used in photoresist lithography for tiny feature structuring [2–5]. Compared with nanosecond pulsed lasers, femtosecond laser has important advantages of extremely high laser peak intensity and small heat affected zone for high quality surface nanostructuring.

Combining unique features of femtosecond laser and NSOM, different patterns can be produced on a spin-coated thin film of UV photoresist. With different laser powers and exposure time, pattern sizes (width and depth) vary greatly. In this paper, the effect of probe-to-sample distance is discussed. Three nano-patterned shapes of dumbbell, ellipsoid, and circle are observed at different probe-to-sample distances. Numerical simulation of laser light intensity distribution across the NSOM probe based on the Bethe–Bouwkamp model shows that there are different light intensity distribution at different probe-to-sample distances, which agrees well with our experimental results. Nanoline patterns with a width of 20 ± 5 nm, which are a half of the fiber probe aperture size and 1/20 of irradiation laser wavelength, are achieved.

2. Experimental setup

The photoresist thin film used in this study is ma-P 1205 (MicroResist), which is sensitive to light irradiation ranging

* Corresponding author. Tel.: +65 68748707; fax: +65 67771349.
E-mail address: Hong_Minghui@dsi.a-star.edu.sg (M.H. Hong).

0924-4247/$ – see front matter © 2006 Elsevier B.V. All rights reserved.
doi:10.1016/j.sna.2006.05.047

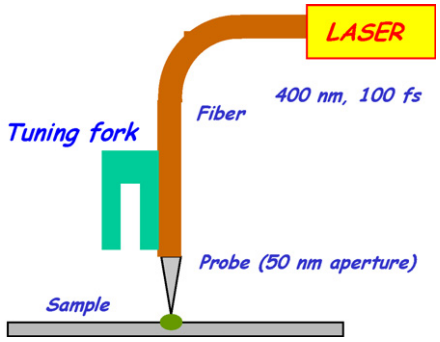

Fig. 1. Schematic drawing of experimental setup for femtosecond laser/NSOM nano-lithography.

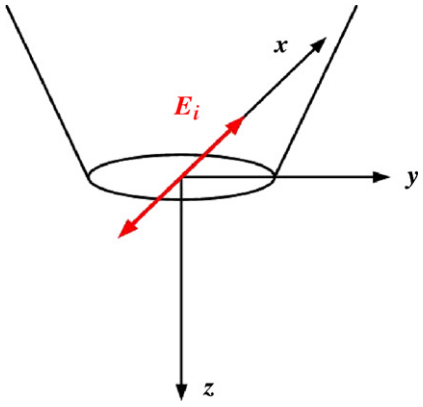

Fig. 2. Schematic diagram of the coordinate system used in the calculation.

from 300 to 400 nm. It was spin-coated on a cleaned silicon substrate by a series of spin coating processes: Firstly, a thin layer Hexamethiyl disialne (HDMS) primer was deposited. Then photoresist (diluted with thinner T-1050 by a factor of 1:4) was spin-coated at a rotation speed of 6000 rpm. Finally, the sample was baked at an environment temperature of 100 °C for 30 s. The final film thickness got is around 40 nm. Fig. 1 shows the experimental setup for the femtosecond laser/NSOM nanolithography. Laser beam from a second-harmonic generation of femtosecond laser (Specra-physics, 400 nm and 100 fs, pulse repetition rate of 80 MHz) was coupled into a NSOM (Aurora-2, Veeco) probe fiber through a 15 m long fiber (Einst, PCS fiber). After the laser nano-patterning, the sample was put into a developer ma-D 331 (Micro Resist) for 20 s, washed in DI water, and then dried by nitrogen gas. The sample was characterized by a scanning electron microscopy (SEM Hitachi S4100) and the profiles were also measured by atomic force microscopy (AFM DI3000).

3. Theoretical study

A rigorous calculation of the emission electromagnetic field from a small aperture of probe has not been solved yet though there were many models developed up to now. The simplest model for an aperture probe is to suppose that the properties of optical fiber probe to that produced by monochromatic light incident upon a subwavelength circular hole in a perfectly conducting metallic screen [8].

More realistic models about field distribution from NSOM probe have been proposed, such as multiple–multipole method [9] and finite-difference time-domain (FDTD) method [10]. But these methods are quite complicated and restricted to 2D studies due to time and memory constraints. To illustrate the experimental results in Section 4, Bethe–Bouwkamp model is used for tip emission simulation in this paper.

Here the NSOM probe is considered as a circular aperture of radius a in a perfectly metallic thin screen. The aperture plane is in the x–y plane. The incident field arrives along the z-axis and is polarized along the x axis, and its amplitude is E_i, as shown in the Fig. 2. Making the original of the coordinates at the center of the aperture, the electric field in the aperture is given by [8]:

$$\left[E_0(x,y)\right]_x = -\frac{4ik_0}{3\pi}\frac{2a^2-x^2-y^2}{(a^2-x^2-y^2)^{1/2}}E_i,$$

$$\left[E_0(x,y)\right]_y = -\frac{4ik_0}{3\pi}\frac{xy}{(a^2-x^2-y^2)^{1/2}}E_i$$

This gives:

$$[E_0(\vec{k})]_x = -\frac{8ik_0a^3E_i}{3}\left(-\cos(\mathrm{ak})\frac{3k_y^2}{a^2k^4}+\sin(\mathrm{ak})\frac{a^2k_x^4+3k_y^2+a^2k_x^2k_y^2}{a^3k^5}\right),$$

$$[E_0(\vec{k})]_y = -\frac{8ik_0a^3E_i}{3}\left(\cos(\mathrm{ak})\frac{3k_xk_y}{a^2k^4}+\sin(\mathrm{ak})\frac{k_xk_y(-3+a^2k_x^2+a^2k_y^2)}{a^3k^5}\right)$$

probe can be described as a small circular aperture in a metallic screen, which is a classic problem in diffraction theory. The well-known Kirchhoff approximation is to suppose that the field in the aperture is the incident field. This approximation, however, is no longer valid when the diameter of aperture is smaller than wavelength because the boundary conditions cannot be solved. In 1944, Bethe [6] presented a more rigorous method: the diffracted field was derived from a fictitious magnetic charge and currents in the hole. And in 1950, Bouwkamp [7] improved Bethe's equations for the near field. So Bethe–Bouwkamp model approximates the radiation emitted from a tapered metal-coated

where $k_0 = 2\pi/\lambda$ is wave vector of laser light from a near-field probe, $k = (k_x, k_y)$ wave vector of laser across probe. The electric field at a point r in a vacuum is given by

$$\vec{E}_v(x,y,z) = \frac{1}{4\pi^2}\iint \vec{E}_v(\vec{k},z)\exp(i\vec{k}\cdot\vec{r})\mathrm{d}\vec{k}$$

where $\vec{E}_v(\vec{k},z) = \vec{E}_0(\vec{k})\exp(izk_v(\vec{k}))$,

$$k_v(\vec{k}) = \sqrt{k_0^2-k^2}.$$

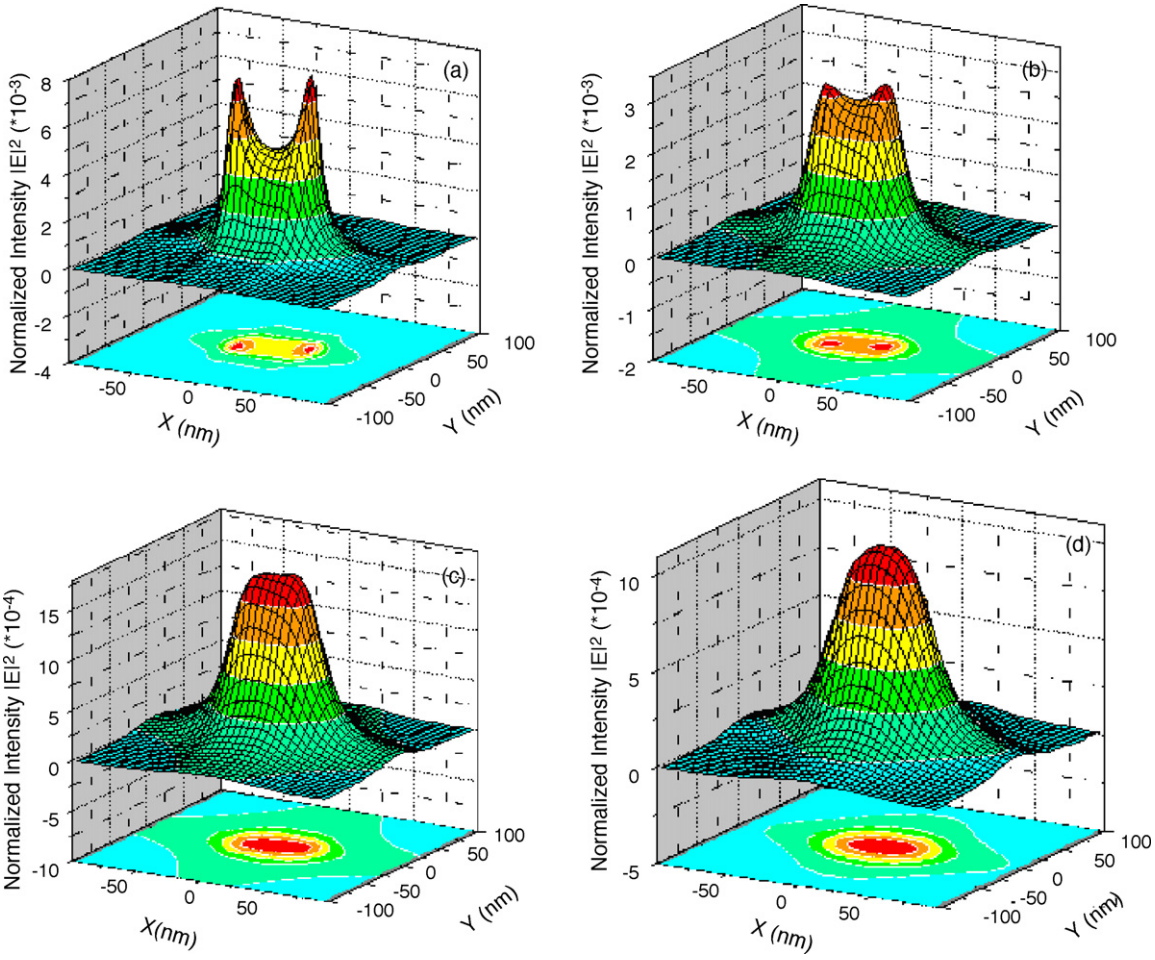

Fig. 3. 3D and bottom contour images of light intensity distributions across an NSOM probe at the probe-to-sample distances of (a) 5 nm, (b) 10 nm, (c) 15 nm and (d) 20 nm.

This electric field equation gives rise to both evanescent ($k^2 > k_0^2$) and propagating waves ($k^2 < k_0^2$). In near-field zone, the strength of evanescent field clearly exceeds propagating one. But these two fields cannot be separated physically and they both contribute to laser process. Therefore, the simulation following is the calculating result of evanescent and propagating field together.

Fig. 3 shows the simulation results of light intensity distribution along x–y planes at different distances of (a) 5 nm, (b) 10 nm, (c) 15 nm, and (d) 20 nm to the sample surface. It is clear that the light intensity distribution varies greatly with different probe-to-sample distances. At a small distance (smaller than 10 nm) double-peak intensity generates. And with increasing distance, double-peak is replaced by single-peak and peak intensity decreased (from 10^{-3} order to 10^{-4}). There is also difference for single-peak intensity distribution: the bottom contour images changes from ellipse to circle shape.

4. Results and discussion

Making use of femtosecond laser/NSOM set-up, different nano-patterns can be designed and produced, such as line-and-space period, dot arrays, and orthogonal gratings. Fig. 4 shows positive and negative MOS patterns produced by the femtosecond laser/NSOM nano-lithography approach with the full width at half maximum (FWHM) of a channel line around 80 nm (positive) and 400 nm (negative).

From the light intensity distribution simulation according to Bethe–Bouwkamp, it is found that probe-to-sample distance should affect the pattern features greatly. In this section, the effect of probe-to-sample distance on pattern feature size was discussed. In NSOM systems the shear-force method is widely applied to control the probe approaching the sample surface [11,12]. For our NSOM system, shear force feedback is represented as a set-point value at the operation panel, which is varied to change the probe-to-sample distance. The set-point value is not set constant at operation. At first, one set-point value was set according to feedback signal and made the probe approach the sample automatically. To reduce the probe-to-sample distance further, set-point value was increased gradually while avoiding crash sample. The difference of the set-point values during the probe approaching process is called “set-point gain” hereafter. To make the probe closer to the sample, the set-point gain would be higher. To study the probe-to-sample distance effect on laser nano-patterning results, dot-patterns are produced with different set-point gains at a same laser power in this paper.

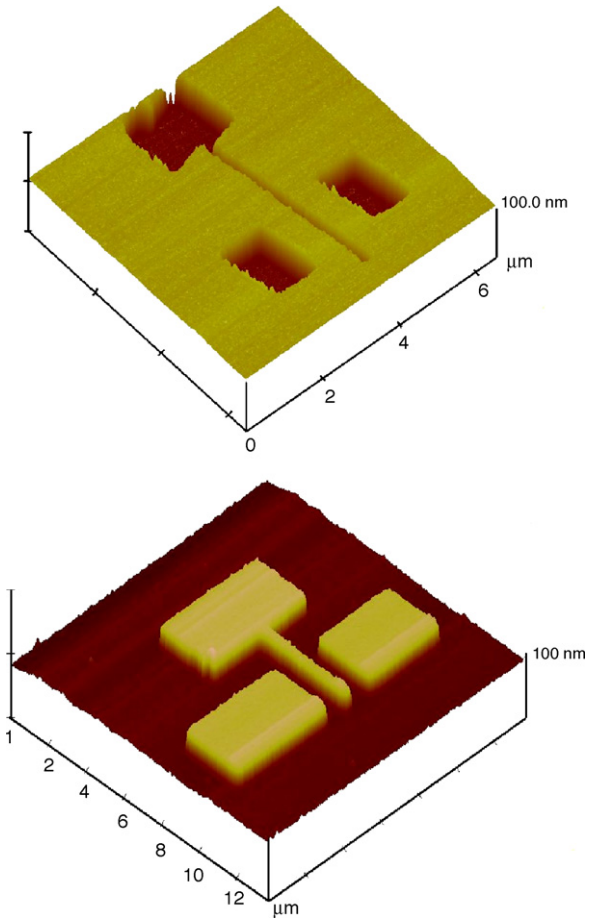

Fig. 4. Positive and negative MOS patterns produced by NSOM.

Fig. 5 shows dot array patterns with different set-point gains and exposure time but same laser power coupling to probe. Since the probe-to-sample distance increases with reducing set-point gain, the distance for pattern (b) is smaller than pattern (a). The line profiles show that photoresist have been both exposed through to the substrate surface for two patterns, but the shapes are much different. The dot cross shape in Fig. 5(a) is like "V" shape, while one plane appears at dot bottom in Fig. 5(b), which is like inverse trapezoid. The plane appearing at the bottom implies that at smaller probe-to-sample distance there was more energy arriving at and exposing the sample although the exposure time is shorter. Therefore, probe-to-sample distance plays a greater effect than exposure time on pattern structure.

It is also found in our study that at the same laser power and exposure time, different probe-to-sample distance will lead to different shapes of dot patterns. Fig. 6 shows the 3D AFM images produced at the same laser power (0.02 mW coupled into NSOM probe) and exposure time (100 ms), but at different set-point gains of (a) 3.9 nA, (b) 2.5 nA and (c) 1.5 nA, which corresponded to smallest probe-to-sample distance for (a) and largest for (c). There are three kinds of dot pattern shapes generated: dumbbell, ellipsoid and circle, with increasing probe-to-sample distance.

Such distinctive dot-patterns shapes at different probe-to-sample distances should be due to different light intensity distri-

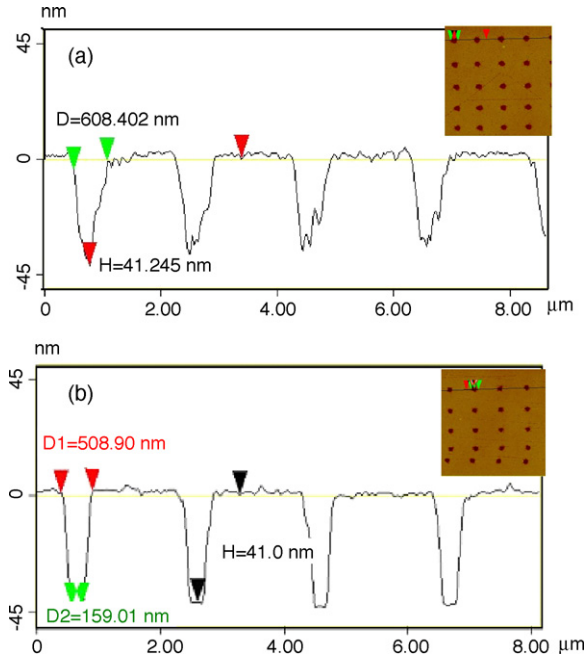

Fig. 5. Line profiles and AFM images of dot arrays with exposure time and set-point gains of (a) 150 ms, 1.1 nA and (b) 100 ms and 1.5 nA.

butions under the NSOM probe. Compare the dot patterns with light intensity distribution simulation in Section 3, it is found that the peak shapes of the light intensity across the NSOM probe agree well with the dot pattern shapes obtained in the experiment. It is believed that the double-peak and ellipse-peak intensity result in dumbbell and ellipsoid dot pattern shapes, respectively. Since it is difficult to detect the accurate probe-to-sample distance at operation, the exact relationship between

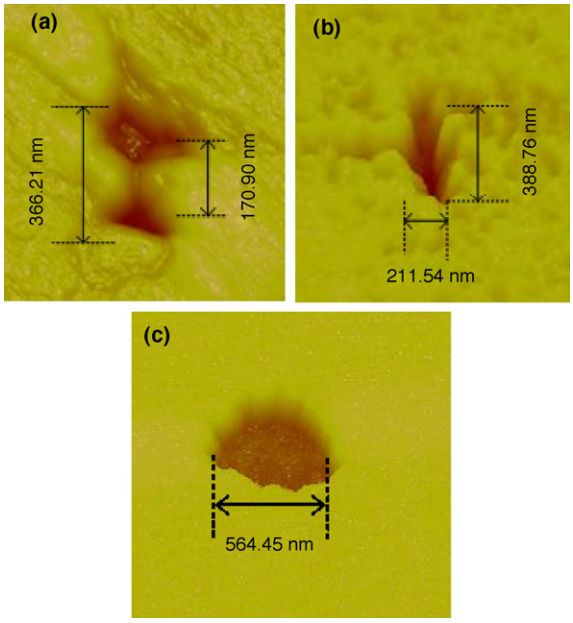

Fig. 6. 3D AFM images at a laser power of 0.02 mW (coupled into NSOM probe), an exposure time of 100 ms and the set-point gains of (a) 3.9 nA, (b) 2.5 nA and (c) 1.5 nA.

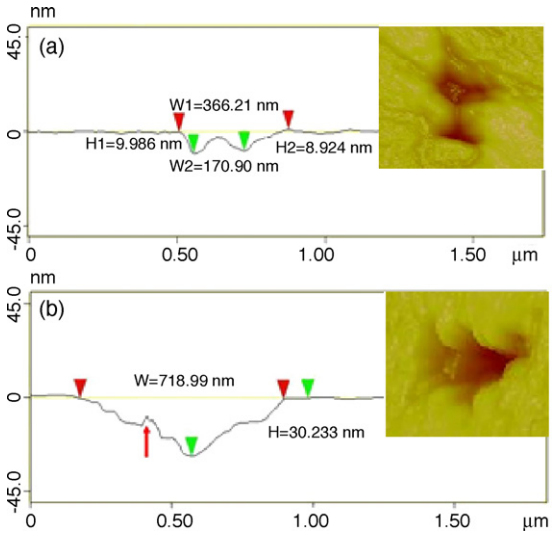

Fig. 7. Line profiles and 3D AFM images of dumbbell shape dots produced at the exposure time of (a) 100 ms and (b) 200 ms.

distance and set-point gain cannot be told. From the comparison between theoretical simulation and experimental results, however, it is proved that probe-to-sample distance decreases with larger set-point gain.

It is also found that these special dot patterns, dumbbell and ellipsoid, were obtained only when laser power and exposure time were low enough. Fig. 7 shows line profiles and 3D AFM images of dumbbell dot pattern with different exposure time (a) 100 ms and (b) 200 ms while keeping laser power and probe-to-sample distance unchanged. Dumbbell shape has been unclear at longer exposure time although the edge between two holes still can be told. The ellipsoid shape will also become circle shape if exposure time or laser power is large.

Besides the probe-to-sample distance, laser power and exposure time also affect the patterns created [13]. It was found that larger laser power and longer exposure time lead to larger pattern size (width and depth). With fine tuning of the laser power and the writing speed, sub-30 nm feature size can be achieved. Fig. 8 shows nano-line with a width of 20 ± 5 nm. It is at a resolution of $\lambda/20$ (λ: laser wavelength) and $a/2$ (a: NSOM probe aperture

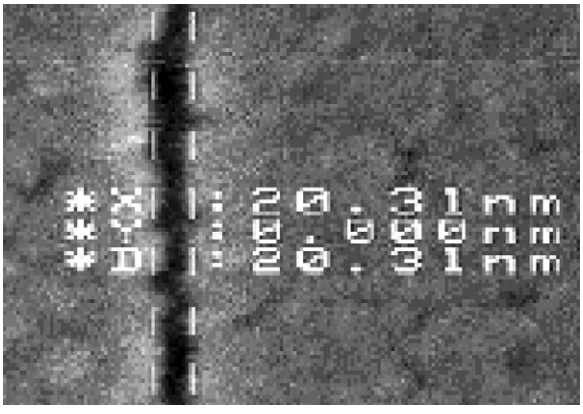

Fig. 8. SEM image of the nano-sized line created by femtosecond laser/NSOM nanolithography.

diameter), respectively. Such high resolution can be compared with E-beam lithography and be used for ultrahigh density data storage.

5. Conclusions

Integration of NSOM and femtosecond laser can produce near-field optical nanolithography on the UV photoresist. It is found that laser power, exposure time and probe-to-sample distance affect the pattern feature sizes greatly. Furthermore, the probe-to-sample distance not only affects the pattern size, but also leads to different pattern shapes, which is proved by the experimental results and theoretical simulation. By proper tuning of the nanolithography processing parameters, sub-30 nm resolution can be obtained. With a smaller aperture NSOM probe and higher order non-linear effect optical crystals for shorter femtosecond laser wavelength, this lithography resolution would be pushed down further to around 10 nm for a high resolution optical detection and nanoprocessing.

References

[1] S. Davy, M. Spajer, Near field optics: snapshot of the field emitted by a nanosource using a photosensitive polymer, Appl. Phys. Lett. 69 (1996) 3306–3308.
[2] S. Maruo, O. Nakamura, S. Kawata, Three-dimensional microfabrication with two-photon-absorbed phhotopolymerization, Opt. Lett. 22 (1997) 132–134.
[3] G. Witzgall, R. Vrijen, E. Yablonovitch, V. Doan, B.J. Schwartz, Single-shot two-photon exposure of commercial photoresist for the production of three-dimensional structures, Opt. Letter. 23 (1998) 1745–1747.
[4] B.H. Cumpston, Two-photon polymerization initiators for three-dimensional optical data storage and microfabrication, Nature 398 (1999) 51–53.
[5] S. Kawata, H.-B. Sun, T. Tanaka, K. Takada, Finer features for functional microdevices, Nature 412 (2001) 697–698.
[6] H.A. Bethe, Theory of diffraction by small holes, Phys. Rev. 66 (1944) 163–182.
[7] C.J. Bouwkamp, Diffraction theory, Rep. Phys. 27 (1954) 35–100.
[8] R. Stevenson, D. Richards, The use of a near-field probe for the study of semiconductor heterostructures, Semicond. Sci. Technol. 13 (1998) 882–886.
[9] L. Novotny, D.W. Pohl, P. Regli, Light propagation through nanometer-sized structures: the two-dimensional-aperture scanning near-field optical microscope, J. Opt. Soc. Am. A 11 (1994) 1768–1779.
[10] H. Furukawa, S. Kawata, Analysis of image formation in a near-field scanning optical microscope: effects of multiple scattering, Opt. Commun. 132 (1996) 170–178.
[11] I.I. Smolyaninov, D.L. Mazzoni, C. Davis, Near-field direct-write ultraviolet lithography and shear force microscopic studies of the lithographic process, Appl. Phys. Lett. 67 (1996) 3859–3861.
[12] O. Bergossi, M. Spajer, P. Schiavone, Visualization of latent images by reflection near field optical microscopy, Ultramicroscopy 61 (1995) 241–246.
[13] Y. Lin, M.H. Hong, W.J. Wang, Y.Z. Law, T.C. Chong, Sub-30 nm lithography with near-field scanning optical microscope combined with femtosecond laser, Appl. Phys. A 80 (2005) 461–465.

Biographies

Ms. Ying Lin received her BE (2000) degree from Shandong University in China. She is currently a research engineer in Nanoscience and Nanotechnology Initiative, National University of Singapore now. Her research interests are in

the areas of laser assisted nanostructure fabrication and application in optical data storage.

Dr. Ming Hui Hong received his BS and MS from Physics Department, Xiamen University in 1985 and 1988. After teaching in Xiamen University from 1988 to 1994, he continued his ME (1996) and PhD (2000) study in National University of Singapore. Currently, he is a research scientist and an Assistant professor of Electrical and Computer Engineering Department, National University of Singapore. His research interest includes laser ablation and its applications in microprocessing and nanofabrication.

Ms. Wei Jie Wang received her ME degree from National University of Singapore in 1999. She is now employed as senior research engineer by Data Storage Institute in Singapore. Her work focuses on the laser-based micro/nanoprocessing, the development of memory device fabrication and the studying of device physics.

Dr. Zeng Bo Wang received his BSc and MSc degrees in physics from Xiamen University in 1997 and 2001, and the PhD in electrical and computer engineering from National University of Singapore in 2005. He is currently a senior research fellow of Data Storage Institute, Singapore. His current research interests are Near-field Optics and Plasmonics.

Dr. Guo Xin Chen received his BS degree from Nanjing University in 1997 and his PhD from National University of Singapore in 2005. He is now a postdoctoral research fellow at Nanoscience and Nanotechnology Initiative of National University of Singapore. His research interests include nanofabrication, laser micro/nanoprocessing, nonlinear optics and near-field optics.

Dr. Qiong Xie obtained her BE from Hua Zhong University of Science and Technology (HUST, China) in Department of Automatic Control in 1992 and PhD in Physical Electronics from State Key Laboratory of Laser Technology (HUST, China) in 1999. She is a Senior Research Engineer in Data Storage Institute of A*STAR in Singapore. Her research interests are in the area of laser precision microfabrication, nanotechnology and system integration.

Prof. Leng Seow Tan obtained his BE (Hons) from the University of Singapore, ME from the National University of Singapore, and PhD from the University of Hawaii, USA, all in the field of electrical engineering. He is an associate professor in the Department of Electrical and Computer Engineering, National University of Singapore. His research interests are in the areas of compound semiconductor materials and devices, nanostructure fabrication and engineering education.

Prof. Tow Chong Chong obtained his BE degree from the Tokyo Institute of Technology, his ME degree from the National University of Singapore, and his ScD degree from the Massachusetts Institute of Technology, all in Electrical Engineering. He is currently the Director of the Data Storage Institute under the Agency for Science, Technology & Research. Prof. Chong's research interest is in the field of magnetic and optical data storage, especially in advance thin films for ultrahigh-density recording. He is also a Full Professor with Department of Electrical and Computer Engineering, NUS.